Conformal Invariance in Incommensurate Phases

Hyunggyu Park[1,2] **and Mike Widom**[1]

We study finite-size corrections to the free energy of free-fermion models on a torus with periodic, twisted, and fixed boundary conditions. Inside the critical (striped-incommensurate) phase, the free energy density $f(N, M)$ on an $N \times M$ square lattice with periodic (or twisted) boundary conditions scales as $f(N, M) = f_\infty - A(s)/(NM) + \cdots$. We derive exactly the finite-size-scaling (FSS) amplitudes $A(s)$ as a function of the aspect ratio $s = M/N$. These amplitudes are universal because they do not depend on details of the free-fermion Hamiltonian. We establish an equivalence between the FSS amplitudes of the free-fermion model and the Coulomb gas system with electric and magnetic defect lines. The twist angle generates magnetic defect lines, while electric defect lines are generated by competition between domain wall separation and system size. The FSS behavior of the free-fermion model is consistent with predictions of the theory of conformal invariance with the conformal charge $c = 1$. For instance, the FSS amplitude on an infinite cylinder with fixed boundary conditions is found to be one-quarter of that with periodic boundary conditions. Finally, we conjecture the exact form of the FSS amplitudes for an interacting-fermion model on a torus. Numerical calculations employing the Bethe Ansatz confirm our conjecture in the infinite-cylinder limit.

KEY WORDS: Conformal invariance; incommensurate phases; finite-size-scaling amplitudes; free-fermion model; electric and magnetic defect; Coulomb gas; interacting fermion model; Bethe ansatz.

1. INTRODUCTION

Study of finite-size corrections to the free energy of statistical systems is motivated by two facts. First, by understanding the corrections, one can subtract them from finite-size data obtained through transfer matrix or Monte Carlo calculations to obtain the bulk free energy. Second, the finite-size corrections contain information about universality class for systems at

---

[1] Department of Physics, Carnegie-Mellon University, Pittsburgh, Pennsylvania 15213.
[2] Present address: Department of Physics, Boston University, Boston, Massachusetts 02215.

a conformally invariant critical point. Thus, from a utilitarian standpoint, one may improve numerical convergence of finite-size data if universality class is known. Or one may determine the universality class by measuring the finite-size effects.

A great deal is known about finite-size effects in a variety of systems.[1–3] The form of corrections to the free energy depends on dimensionality, universality class, geometry, boundary conditions, and whether the system is at a critical point, but is independent of further details for a wide class of models. Perhaps the most significant result is a universal formula for corrections to the free energy at conformally invariant critical points in two dimensions.[4] Consider a strip of finite width N and infinite height, which is the usual geometry for transfer matrix calculations. With free (or fixed) boundary conditions across the strip, the free energy takes the form

$$f_N = f_\infty + f_s/N - (\pi/24)\, \zeta c/N^2 + \cdots \tag{1}$$

where f_s is a nonuniversal surface free energy associated with strip boundaries, ζ is the *anisotropy factor* (the scale factor by which the vertical axis must be multiplied to achieve rotational invariance of correlation functions), and c is the *conformal charge* defining the universality class of the system.[5]

When periodic boundary conditions are utilized, the form changes slightly. Now $f_s = 0$ and the coefficient of the second-order correction (finite-size-scaling amplitude) is exactly four times larger,

$$f_N = f_\infty - (\pi/6)\, \zeta c/N^2 + \cdots \tag{2}$$

The anisotropy factor can often be isolated by running the transfer matrix in the perpendicular direction. That is, in a system of infinite width N but finite height M, Eq. (2) becomes[6]

$$f_N = f_\infty - (\pi/6\zeta)\, c/M^2 + \cdots \tag{3}$$

We actually calculate the finite-size corrections for systems which are rectangular, with height M and width N, as a function of the aspect ratio $s = M/N$. Thus, our results include the limiting geometries of Eqs. (2) and (3). Furthermore, the finite-aspect-ratio cases may be of use in analyzing results of Monte Carlo calculations[7] as well as transfer matrix studies.

Many important models of statistical mechanics (e.g., Ising and Potts models) acquire conformal invariance at their critical points. Thus, Eqs. (1)–(3) can be applied once the conformal charge is determined. There are, however, a few problems (e.g., directed percolation) lacking conformal

invariance for which the universal formulas should not hold. One impor-
tant set of models for which questions of conformal invariance and finite-
size corrections have not been thoroughly investigated are those displaying
incommensurate phases[8] (e.g., ANNNI and chiral 3-state Potts models).
This paper represents a first step toward filling that gap.

In this paper we study fermion models without dislocations. Figure 1
shows a prototypical two-dimensional striped-incommensurate phase.
Domain walls run vertically on average. Without dislocations the number
of walls is a conserved, integral value with periodic boundary conditions.
In the models considered in this paper the entire incommensurate phase is
a critical phase with continuously varying domain wall density d. Domain
wall density correlation functions decay algebraically with a modulation
such that domain walls are placed periodically at distances $l_h = 1/d$ on
average.

We want to know if the formulas of conformal invariance hold. Space
is clearly anisotropic, since the domain walls always run vertically on
average. Isotropy must be regained by a simple anisotropy factor if
Eqs. (1)–(3) are to hold. Scale invariance requires that there be no significant
length scale in a system except for the correlation length, which must be
infinite. The microscopic lattice constant, for example, is usually an irrelevant
length. In incommensurate systems there is a third length, the domain wall
separation l_h, to be concerned with. This length must be irrelevant in some
sense for conformal invariance to hold. Thus, there is a significant reason
to question whether Eqs. (1)–(3) apply to incommensurate phases.[9, 10]

The principal result of this paper is that these equations do hold in the
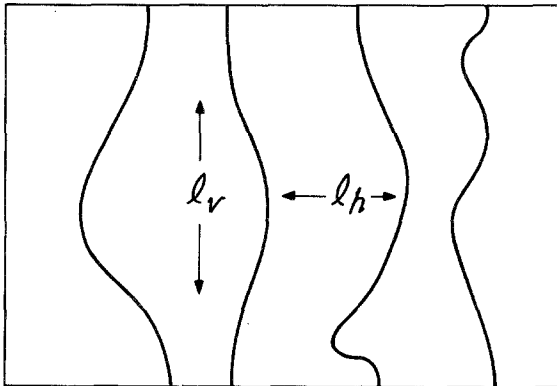

Fig. 1. A domain-wall configuration of a striped-incommensurate phase. Domain walls are
denoted by vertical wiggly lines. The horizontal length scale l_h represents the average domain
wall separation and the vertical length scale l_v represents the average vertical distance between
collisions of domain walls.

incommensurate phase if one takes into account an *electric defect* generated by competition between the domain wall separation l_h and the system size N. Physically, this defect arises because the bulk domain wall density d is incompatible in general with any finite system size. That is, the number of domain walls expected to occur in a system of width N is Nd. This value is usually not an integer, but periodic boundary conditions allow only integral numbers of domain walls to be present. So the system is forced out of its normal ground state by the conservation of domain wall number. The magnitude (charge) of the defect is the number of missing domain walls. Because of this defect, care must be taken in extrapolating finite-size data to bulk values and extracting finite-size behavior of the free energy. We also show that the twist angle in twisted boundary conditions generates a *magnetic* defect line. The electric and magnetic defects are dual to each other.

Our results follow from calculating the exact finite-size-scaling (FSS) amplitudes of the free fermion model on a torus using an asymptotic expansion method. These amplitudes are universal. That is, they do not depend on details of the free-fermion dispersion relation. In fact, we find they are equivalent to those of the six-vertex model (or the Coulomb gas[11]) with electric and magnetic defect lines. In the infinite-cylinder limits ($s \to \infty$ and $s \to 0$), we show that Eqs. (2) and (3) hold and the conformal charge $c = 1$. But the presence of the defects leads to an effective $c < 1$ in the $s \to \infty$ limit. With fixed boundary conditions we confirm that Eq. (1) holds.

Next, we extend our results to an interacting-fermion model. The symmetric six-vertex model is equivalent to an interacting fermion model at the half-filling in the time-continuum limit. The FSS amplitudes of this vertex model are known exactly on a torus.[12,13] The incommensurate phase of the free-fermion model has a continuously varying domain wall density. Comparing these amplitudes of the free-fermion model and the half-filled interacting-fermion model, we conjecture the exact form of the FSS amplitudes of the non-half-filled interacting-fermion model on a torus (the incommensurate phase with interacting domain walls). Employing the Bethe Ansatz, we confirm our conjecture numerically in the infinite-cylinder limit. Analytic perturbation calculations in certain limits also confirm our conjecture. Some of our results have been published elsewhere[14] and this paper provides details and complete results.

The remainder of the paper is organized as follows. In Section 2, we introduce the free-fermion model and solve it on toroidal lattices of finite size. Then the solution is used to compute the finite-size corrections to the free energy in Section 3. In Section 4, we extend our results to an interacting-fermion model. Finally, we discuss our results.

2. THE FREE FERMION MODEL

Consider a two-dimensional statistical model on a square lattice with horizontal width N and vertical height M. Let $s_m(n)$ be a statistical variable defined at site (n, m) where $n = 1, 2,..., N$ and $m = 1, 2,..., M$. The Hamiltonian of the system H is written as the sum of interaction Hamiltonians between statistical variables of neighboring rows, i.e., $H = \sum_m H(s_m, s_{m+1})$, where $s_m = \{s_m(1),..., s_m(N)\}$. For simplicity, only nearest-neighbor interactions are considered. In the vertical direction, periodic boundary conditions are taken throughout this paper, $s_{M+1} = s_1$. Then the partition function is

$$\mathscr{Z} = \sum_{s_1, s_2, ...} \exp\left[-\sum_{m=1}^{M} H(s_m, s_{m+1}) \right]$$
$$= \mathrm{Tr}\, \mathscr{T}^M \tag{4}$$

where the transfer matrix $\mathscr{T}$ is defined as $\langle s | \mathscr{T} | s' \rangle = \exp[-H(s, s')]$.

Two-dimensional statistical models can be described by one-dimensional quantum field theories. By defining the quantum Hamiltonian as $\mathscr{H} = -\ln(\mathscr{T})$, we obtain for the partition function

$$\mathscr{Z} = \mathrm{Tr}\, \exp(-M\mathscr{H}) \tag{5}$$

The transfer matrix $\mathscr{T}$ can be interpreted as a time-evolution operator of a one-dimensional quantum mechanical system by viewing the vertical axis as the time direction. It is generally difficult to find exact quantum Hamiltonians corresponding to well-known classical statistical models, because of noncommutativity between operators in transfer matrices. Instead they are obtained only in the anisotropic limit (time-continuum limit). However, these Hamiltonians in the time-continuum limit usually sustain universal features of the nature of phases and phase transitions, including finite-size scaling.

Consider the simple quantum Hamiltonian

$$\mathscr{H} = m \sum_{n=1}^{N} \sigma_n^+ \sigma_n^- - \frac{t}{2} \sum_{n=1}^{N} (\sigma_n^+ \sigma_{n+1}^- + \sigma_n^- \sigma_{n+1}^+) \tag{6}$$

where $\sigma_n^{\pm}$ are the Pauli-spin raising/lowering operators at site n. This Hamiltonian describes a simple domain wall model on a two-dimensional square lattice. The spin-up state ($\sigma_n^z = +1$) is identified with presence of a domain wall at site n and the spin-down state ($\sigma_n^z = -1$) with vacancy. Then $\sigma_n^{\pm}$ serve as the creation/annihilation operators of a domain wall at site n. Here m is the energy (or mass) of the domain wall and t the nearest-

neighbor hopping probability. The Pauli exclusion principle guarantees no meetings of domain walls. This quantum Hamiltonian does not allow pair-creation/annihilation of domain walls or back bendings (no dislocations). Domain walls must extend from the bottom edge to the top in the vertical direction, so the number of domain walls is conserved. Domain walls may hop to further-neighboring sites as well as nearest neighbors with probability of order t^{d_h} (d_h is the hopping distance). The partition function $\mathscr{Z}$ [Eq. (5)] includes these multiple-hoppin terms from the expansion of $\exp(-\mathscr{H})$. Notice that the domain-wall quantum Hamiltonian at $m = 0$ is identical to that of the six-vertex model at the so-called *free-fermion* point, i.e., the Hamiltonian of the *XXZ* quantum chain at $\Delta = 0$.[15]

The Pauli spin operators $\sigma_n^{\pm}$ satisfy the fermion-anticommutation relation at the same site, $\{\sigma_n^{+}, \sigma_n^{-}\} = 1$, but commute at different sites. Genuine fermions which anticommute at different sites can be generated by the Jordan–Wigner transformation

$$a_n^{\pm} = \sigma_n^{\pm} \exp\left(i\pi \sum_{m=1}^{n-1} \sigma_m^{+}\sigma_m^{-}\right) \tag{7}$$

for $n = 1, 2, ..., N$. The phase factor counts the number of domain walls to the left of the site n and ensures the anticommutativity of fermions at different sites, $\{a_n^{+}, a_m^{-}\} = \delta_{nm}$. We assign an additional minus sign to the definition of $a_{N+1}^{\pm}$, i.e.,

$$a_{N+1}^{\pm} = -\sigma_{N+1}^{\pm}(-1)^{n_d} \tag{8}$$

where n_d is the number of domain walls in the system. Recall that the number of domain walls is conserved and therefore serves as a good quantum number. With these transformations, the quantum Hamiltonian, Eq. (6), may be rewritten as

$$\mathscr{H} = m \sum_{n=1}^{N} a_n^{+} a_n^{-} - \frac{t}{2} \sum_{n=1}^{N} (a_n^{+} a_{n+1}^{-} - a_n^{-} a_{n+1}^{+}) \tag{9}$$

We now compute the free energy of this system with periodic, twisted, and fixed boundary conditions. First, we consider periodic boundary conditions in terms of domain walls in the horizontal direction, i.e., $\sigma_{N+1}^{\pm} = \sigma_1^{\pm}$. From Eq. (8), the fermion operators satisfy

$$a_{N+1}^{\pm} = -a_1^{\pm}(-1)^{n_d} \tag{10}$$

The eigenstates of this Hamiltonian are plane waves,

$$a_k^{\pm} = \frac{1}{\sqrt{N}} \sum_{n=1}^{N} a_n^{\pm} \exp(\pm ikn) \tag{11}$$

and the Hamiltonian becomes

$$\mathscr{H} = \sum_{j=1}^{N} \mathscr{E}(k_j)\, a_{k_j}^{+}\, a_{k_j}^{-} \tag{12}$$

where the dispersion relation is given as $\mathscr{E}(k) = m - t\cos(k)$. From the boundary conditions, Eq. (10), the wavevector k takes N discrete values between $-\pi$ and π satisfying

$$\exp(ik_j N) = \begin{cases} 1 & \text{if } n_d = \text{odd integer} \\ -1 & \text{if } n_d = \text{even integer} \end{cases} \tag{13}$$

In case of N even, $k_j = (\pi/N)(2j - N)$ for odd n_d and $k'_j = (\pi/N)(2j - 1 - N)$ for even n_d $(j = 1,..., N)$. For convenience, we denote $k = \{k_j\}$ and $k' = \{k'_j\}$.

The partition function on a square lattice with periodic boundary conditions in both directions (a torus) splits into two sectors (odd and even n_d),

$$\mathscr{Z} = \sum_{\substack{n_k = 0,1 \\ \sum_k n_k = \text{odd}}} \exp\left[-M\sum_k \mathscr{E}(k)n_k\right] + \sum_{\substack{n_{k'} = 0,1 \\ \sum_{k'} n_{k'} = \text{even}}} \exp\left[-M\sum_{k'} \mathscr{E}(k')n_{k'}\right] \tag{14}$$

where n_k $(= 0, 1)$ is the eigenvalue of the number operator $a_k^{+}a_k^{-}$ (i.e., the occupation number of the state with wavevector k). It can be shown that the above partition function $\mathscr{Z}$ is equivalent to the following:

$$\mathscr{Z} = \frac{1}{2}\sum_{i=1}^{4} p_i \mathscr{Z}_i \qquad (p_1 = -1, p_2 = p_3 = p_4 = 1) \tag{15}$$

where

$$\mathscr{Z}_1 = \prod_{j=1}^{N} [1 - \exp(-M\mathscr{E}(k_j))]$$

$$\mathscr{Z}_2 = \prod_{j=1}^{N} [1 + \exp(-M\mathscr{E}(k_j))]$$

$$\mathscr{Z}_3 = \prod_{j=1}^{N} [1 + \exp(-M\mathscr{E}(k'_j))] \tag{16}$$

$$\mathscr{Z}_4 = \prod_{j=1}^{N} [1 - \exp(-M\mathscr{E}(k'_j))]$$

Next, consider twisted boundary conditions defined as $\sigma_{N+1}^{+} = \sigma_{1}^{\pm}$ $\exp(\pm i2\pi\phi)$. These boundary conditions do not produce any surface free energy and change only phase factors of wavefunctions (*gauge-invariant boundary conditions*). Without loss of generality, one may restrict the value of ϕ to lie between $-1/2$ and $1/2$. The fermion operators satisfy

$$a_{N+1}^{\pm} = -a_{1}^{\pm}(-1)^{n_d} \exp(\pm i2\pi\phi) \tag{17}$$

and the wavevectors are shifted to

$$k_j = \begin{cases} \dfrac{\pi}{N}(2\phi + 2j - N) & \text{if } n_d = \text{odd integer} \\[2mm] \dfrac{\pi}{N}(2\phi + 2j - 1 - N) & \text{if } n_d = \text{even integer} \end{cases} \tag{18}$$

for N even. Note that the twist angle shifts the wavevectors uniformly. The partition function can be written as in Eqs. (15) and (16) with the shifted wavevectors.

Finally, consider boundary conditions which require $\sigma_{N+1}^{\pm} = 0$. These boundary conditions are conventionally called *free* boundary conditions because the quantum chain has free ends.[16] However, in this paper we call them fixed boundary conditions because domain walls cannot cross over the boundary and therefore must remain inside of the system. Once a domain wall reaches the boundary, it reflects back to the interior. The boundary plays the role of an infinite energy barrier and particle (domain-wall) wavefunctions vanish at the boundary. These boundary properties are essentially the same as properties of so-called fixed boundary conditions in spin systems and quantum mechanical problems.

With fixed boundary conditions the Hamiltonian (6) becomes

$$\mathcal{H} = m \sum_{n=1}^{N} \sigma_n^{+}\sigma_n^{-} - \frac{t}{2} \sum_{n=1}^{N-1} (\sigma_n^{+}\sigma_{n+1}^{-} + \sigma_n^{-}\sigma_{n+1}^{+}) \tag{19}$$

The number of domain walls is still conserved. The eigenstates are standing waves,

$$a_k^{\pm} = \left(\frac{2}{N+1}\right)^{1/2} \sum_{n=1}^{N} a_n^{\pm} \sin(kn) \tag{20}$$

The boundary conditions $a_{N+1}^{\pm} = 0$ require that wavevectors take discrete values

$$k_j = \frac{\pi j}{N+1} \tag{21}$$

where $j = 1, ..., N$. The partition function with fixed (periodic) boundary conditions in the horizontal (vertical) direction is $\mathscr{Z} = \mathscr{Z}_2$ [see Eq. (16)] with the new k-states as above.

One may consider the system where particles (domain walls) can cross over the boundary, so the number of domain walls is not conserved. The particle wavefunctions spread beyond the boundary. We call these boundary conditions *free* boundary conditions. The Hamiltonian can be written as

$$\mathscr{H} = m \sum_{n=1}^{N} \sigma_n^+ \sigma_n^- - \frac{t}{2} \sum_{n=1}^{N-1} (\sigma_n^+ \sigma_{n+1}^- + \sigma_n^- \sigma_{n+1}^+) - \frac{\gamma}{2} (\sigma_N^+ + \sigma_N^- + \sigma_1^+ + \sigma_1^-)$$

(22)

where the third term represents the creation/annihilation of domain walls at the boundary and γ is the probability of such processes. The number of domain walls is no longer conserved and a continuous k spectrum is expected. The Hamiltonian is not diagonalized simply in the k space. We have studied these free boundary conditions through a random tiling model numerically using the transfer matrix method and the results appear elsewhere.[17]

One can generalize our discussion to systems with more general Hamiltonians than Eq. (6). Most of our results in the following sections describe universal features of free-fermion models. They do not depend on details of the Hamiltonian, but only on a few of the general properties of the dispersion relation. We need only assume that the dispersion relation $\mathscr{E}(k)$ satisfies the following conditions:

1. $\mathscr{E}(k) = \mathscr{E}(-k)$.

2. A monotonically increasing analytic function as $|k|$ is larger, i.e., $\mathscr{E}'(k) > 0$ for $k > 0$.

3. A quadratic shape near $k = 0$, i.e., $\mathscr{E}'(0) = 0$, $\mathscr{E}''(0) > 0$.

4. The density of state is a constant (the distribution of wavevectors k is uniform).

Before studying finite-size effects in the free-fermion model, we review briefly some known properties of this model in the bulk (for a more complete review, see Ref. 8). In the thermodynamic limit, boundary conditions do not matter and the free energy density becomes

$$f_\infty = -\frac{\ln \mathscr{Z}}{NM} = \frac{1}{2\pi} \int_{-k_F}^{k_F} dk \, \mathscr{E}(k)$$

(23)

where the Fermi wavevector k_F is defined by $\mathscr{E}(k_F) = 0$, i.e., $\cos(k_F) = m/t$. When $m/t > 1$, the free energy density is zero and this phase is called the

commensurate-solid phase. In this phase, the domain wall density $d = df/dm$ also vanishes. When $m/t < -1$, all states are occupied $(d = 1)$ and $f_\infty = -m$. This phase is called the closed-packed commensurate-solid phase. When $-1 < m/t < 1$, the states below the Fermi surface are occupied. The free energy is given in Eq. (23) with the domain wall density $d = k_F/\pi$. This phase is called the striped-incommensurate floating-solid phase. This phase is a critical phase in the sense that correlation functions decay algebraically. The critical index of the domain wall density $x = 1$. The modulation in the density-density correlation function implies that domain walls are placed periodically at distances $l_h = 1/d$ on average.

The transition between the commensurate and incommensurate phases at $m = t$ $(k_F = 0)$ is known as the Pokrovsky–Talapov transition.[18] Near the transition from the critical phase (small k_F), the domain wall density behaves like

$$d = \frac{k_F}{\pi} \sim \mu^{1/2} \tag{24}$$

where $\mu = -\mathscr{E}(0)/\mathscr{E}''(0)$ $(= 1 - m/t)$ is the reduced coupling constant. The free energy behaves like

$$f_\infty \simeq \frac{k_F}{\pi} \mathscr{E}(0) \sim -\mu^{3/2} \tag{25}$$

Notice that the free energy has a singular term with the 3/2 power of the reduced variable μ, which is the signature of the Pokrovsky–Talapov transition. The second derivative of the free energy, the specific heat, diverges near the transition from the side of the incommensurate phase with exponent $\alpha = -1/2$.

The free-fermion model is an anisotropic model and domain walls follow the temporal (vertical) direction. This anisotropy shows up in the density–density correlation function when one includes the time (vertical distance) dependence. The anisotropy factor ζ, the ratio of the length scale in the horizontal direction compared to that in the vertical direction, is $\zeta = l_h/l_v = t \sin(k_F)$. The horizontal length scale l_h represents the average domain wall separation. The vertical length scale l_v represents the average vertical distance between collisions of domain walls. The anisotropy factor can be interpreted as the velocity of the particle at the Fermi surface, $\zeta = \mathscr{E}'(k_F)$, which is the proper definition of the anisotropy factor in the conformal theory. Near the Pokrovsky–Talapov transition this factor becomes very small, i.e., the system becomes very anisotropic; $\zeta \sim k_F \sim \mu^{1/2}$. The length scale in the vertical direction l_v goes to infinity much faster than that in the horizontal direction l_h. In fact, $l_h = 1/d \sim \mu^{-1/2}$ and $l_v \sim \mu^{-1}$. This is the nature of the anisotropic scaling at the Pokrovsky–Talapov transition.

3. FINITE-SIZE CORRECTIONS TO FREE ENERGIES IN THE INCOMMENSURATE PHASE

In this section we derive the finite-size-scaling amplitudes of the free energy inside the incommensurate (critical) phase of the free-fermion model. We consider $M \times N$ lattices with periodic, twisted, and fixed boundary conditions. The aspect ratio $s = M/N$ is held constant in the thermodynamic limit. We analyze the partition function by an asymptotic expansion method used by several authors for Ising and dimer models.[19,20]

The partition function of the free-fermion model on a torus with periodic boundary conditions in both directions consists of four terms as shown in Eqs. (15) and (16). For each of the four terms we now obtain the leading finite-size corrections. That is, we extract terms of $\mathcal{O}(1)$ multiplying the bulk partition function. For simplicity we only discuss the case in which the number of sites in the horizontal direction N is an even integer (however, final results do not change for odd N). First consider $\mathscr{Z}_3$,

$$
\begin{aligned}
\mathscr{Z}_3 &= \prod_{j=1}^{N} \left\{ 1 + \exp\left[-M\mathscr{E}\left(\frac{\pi(2j-1-N)}{N} \right) \right] \right\} \\
&= \prod_{j=1}^{N/2} \left\{ 1 + \exp\left[-M\mathscr{E}\left(\frac{\pi(2j-1)}{N} \right) \right] \right\}
\end{aligned}
\tag{26}
$$

Define α by

$$
\mathscr{E}(2\pi\alpha/N) = 0
\tag{27}
$$

i.e., $\alpha = Nk_F/(2\pi)$ is of $\mathcal{O}(N)$. The integer closest to α is denoted by p,

$$
\alpha = p + \tilde{\kappa}
\tag{28}
$$

where $-1/2 < \tilde{\kappa} \leqslant 1/2$. Then, $\mathscr{E}(\pi(2j-1)/N)$ is negative for $j = 1,..., p$ and is positive for $j = p+1,..., N/2$. So the number of domain walls of the ground state in this even sector is $n_d = 2p$. We factor $\mathscr{Z}_3$ into three products

$$
\mathscr{Z}_3 = \mathscr{R}_1 \mathscr{R}_2 \mathscr{R}_3
\tag{29}
$$

where

$$
\begin{aligned}
\mathscr{R}_1 &= \prod_{j=1}^{p} \exp\left[-2M\mathscr{E}\left(\frac{\pi(2j-1)}{N} \right) \right] \\
\mathscr{R}_2 &= \prod_{j=1}^{p} \left\{ 1 + \exp\left[M\mathscr{E}\left(\frac{\pi(2j-1)}{N} \right) \right] \right\}^2 \\
\mathscr{R}_3 &= \prod_{j=p+1}^{N/2} \left\{ 1 + \exp\left[-M\mathscr{E}\left(\frac{\pi(2j-1)}{N} \right) \right] \right\}^2
\end{aligned}
\tag{30}
$$

The exponential terms in two products $\mathscr{R}_2$ and $\mathscr{R}_3$ become small compared to unity as M goes to infinity.

First consider the logarithm of $\mathscr{R}_1$,

$$\ln \mathscr{R}_1 = -2M \sum_{j=1}^{p} \mathscr{E}[\pi(2j-1)/N] \tag{31}$$

Using the Euler–Maclaurin formula, with the aspect ratio $s = M/N$ fixed in the thermodynamic limit, we find

$$\ln \mathscr{R}_1 \simeq -\frac{MN}{\pi} \int_0^{2\pi p/N} dk \, \mathscr{E}(k) + \frac{\pi}{6} s \mathscr{E}' \left(\frac{2\pi p}{N} \right)$$

$$\simeq -\frac{MN}{\pi} \int_0^{k_F} dk \, \mathscr{E}(k) + \left(\frac{\pi}{6} - 2\pi \tilde{\kappa}^2 \right) s \zeta \tag{32}$$

where the anisotropy factor $\zeta = \mathscr{E}'(k_F)$ is the Fermi velocity.

$\mathscr{R}_2$ and $\mathscr{R}_3$ are analyzed by an asymptotic expansion method.[19,20] Here we do not go into details of the rigorous derivation of our results, but give a heuristic derivation. Readers interested in the rigorous proof of our results should refer to refs. 19 and 20. The logarithm of $\mathscr{R}_2$ becomes

$$\ln \mathscr{R}_2 = 2 \sum_{j=1}^{p} \ln \left\{ 1 + \exp \left[M\mathscr{E} \left(\frac{\pi(2j-1)}{N} \right) \right] \right\}$$

$$= 2 \sum_{j=1}^{p} \ln \left\{ 1 + \exp \left[M\mathscr{E} \left(\frac{\pi(2p-2j+1)}{N} \right) \right] \right\}$$

$$= 2 \sum_{j=1}^{p} \ln \left\{ 1 + \exp \left[M\mathscr{E} \left(k_F - \frac{\pi(2j-1+2\tilde{\kappa})}{N} \right) \right] \right\}$$

$$\simeq 2 \sum_{j=1}^{\infty} \ln\{1 + \exp[-\pi s\zeta(2j-1+2\tilde{\kappa})]\} \tag{33}$$

where we expanded $\mathscr{E}(k)$ near the Fermi surface $k = k_F$. Similarly,

$$\ln \mathscr{R}_3 \simeq 2 \sum_{j=1}^{\infty} \ln \left\{ 1 + \exp[-\pi s\zeta(2j-1-2\tilde{\kappa})] \right\} \tag{34}$$

Defining the variables q and z by

$$q = \exp(-\pi s\zeta)$$

$$z = i\pi s\zeta \tilde{\kappa} \tag{35}$$

we can write the product of $\mathscr{R}_2$ and $\mathscr{R}_3$ as

$$\mathscr{R}_2\mathscr{R}_3 \simeq \prod_{j=1}^{\infty} [1 + 2\cos(2z) q^{2j-1} + q^{4j-2}]^2$$

$$= q^{1/6}[\theta_3(z, q)/\eta(q)]^2 \tag{36}$$

where $\theta_3(z, q)$ is the Jacobi theta function of the third kind and $\eta(q)$ is the Dedekind eta function.[21,22] Gathering all three products yields

$$\mathscr{Z}_3 \simeq \exp(-MNf_{\infty})q^{2\tilde{\kappa}^2}\left[\frac{\theta_3(z, q)}{\eta(q)}\right]^2 \tag{37}$$

where f_{∞} is the bulk free energy density defined in Section 2. The calculation of $\mathscr{Z}_4$ follows the steps of Eqs. (29)–(37) with the result

$$\mathscr{Z}_4 \simeq \exp(-MNf_{\infty})q^{2\tilde{\kappa}^2}\left[\frac{\theta_4(z, q)}{\eta(q)}\right]^2 \tag{38}$$

where $\theta_4(z, q)$ is the Jacobi theta function of the fourth kind.[22]

Now consider $\mathscr{Z}_2$. For $\tilde{\kappa} > 0$ ($\tilde{\kappa} < 0$), $\mathscr{E}(2\pi j/N)$ is negative for $j = 1,..., p$ ($j = 1,..., p-1$) and is positive otherwise [see Eqs. (27) and (28)]. The number of domain walls of the ground state in this odd sector is $n_d = 2p + 1$ ($2p - 1$), respectively. Let us consider the case of $\tilde{\kappa} > 0$ first. We factor $\mathscr{Z}_2$ into five products,

$$\mathscr{Z}_2 = \mathscr{R}_0\mathscr{R}_1\mathscr{R}_2\mathscr{R}_3\mathscr{R}_4 \tag{39}$$

where

$$\mathscr{R}_0 = 1 + \exp[-M\mathscr{E}(0)]$$

$$\mathscr{R}_1 = \prod_{j=1}^{p} \exp[-2M\mathscr{E}(2\pi j/N)]$$

$$\mathscr{R}_2 = \prod_{j=1}^{p} \{1 + \exp[M\mathscr{E}(2\pi j/N)]\}^2 \tag{40}$$

$$\mathscr{R}_3 = \prod_{j=p+1}^{N/2-1} \{1 + \exp[-M\mathscr{E}(2\pi j/N)]\}^2$$

$$\mathscr{R}_4 = 1 + \exp[-M\mathscr{E}(\pi)]$$

Applying the Euler–Maclaurin formula as in Eq. (32), we find

$$\ln \mathcal{R}_1 = -2M \sum_{j=1}^{P} \mathscr{E}\left(\frac{2\pi j}{N}\right)$$

$$\simeq -\frac{MN}{\pi} \int_0^{2\pi p/N} dk\, \mathscr{E}(k) - M\left[\mathscr{E}\left(\frac{2\pi p}{N}\right) - \mathscr{E}(0)\right] - \frac{\pi}{3} s\mathscr{E}'\left(\frac{2\pi p}{N}\right) \quad (41)$$

Using the relation $2\pi p/N = k_F - 2\pi\tilde{\kappa}/N$ from Eqs. (27) and (28), we find that $\ln(\mathcal{R}_0 \mathcal{R}_1)$ becomes

$$\ln(\mathcal{R}_0 \mathcal{R}_1) \simeq -MNf_\infty - \left[\frac{\pi}{3} - 2\pi\tilde{\kappa}(1 - \tilde{\kappa})\right] s\zeta \quad (42)$$

Dominant contributions from $\mathcal{R}_2$ and $\mathcal{R}_3$ are

$$\ln \mathcal{R}_2 \simeq 2 \sum_{j=1}^{\infty} \ln\{1 + \exp[-\pi s\zeta(2j - 2 + 2\tilde{\kappa})]\} \quad (43)$$

and

$$\ln \mathcal{R}_3 \simeq 2 \sum_{j=1}^{\infty} \ln\{1 + \exp[-\pi s\zeta(2j - 2\tilde{\kappa})]\} \quad (44)$$

In terms of q and z defined in Eq. (35), the product of $\mathcal{R}_2$ and $\mathcal{R}_3$ is

$$\mathcal{R}_2 \mathcal{R}_3 \simeq \exp(2iz)(2 \cos z)^2 \prod_{j=1}^{\infty} [1 + 2 \cos(2z)\, q^{2j} + q^{4j}]^2$$

$$= \exp(2iz)\, q^{-1/3} \left[\frac{\theta_2(z, q)}{\eta(q)}\right]^2 \quad (45)$$

where $\theta_2(z, q)$ is the Jacobi theta function of the second kind.[22]
    The last term $\mathcal{R}_4 = 1 + \mathcal{O}(e^{-M})$. Therefore

$$\mathcal{Z}_2 \simeq \exp(-MNf_\infty)q^{2\tilde{\kappa}^2} \left[\frac{\theta_2(z, q)}{\eta(q)}\right]^2 \quad (46)$$

We also find

$$\mathcal{Z}_1 \simeq \exp(-MNf_\infty)q^{2\tilde{\kappa}^2} \left[\frac{\theta_1(z, q)}{\eta(q)}\right]^2 \quad (47)$$

where $\theta_1(z, q)$ is the Jacobi theta function of the first kind.[22] When $\tilde{\kappa} < 0$, we find the same results for $\mathcal{Z}_1$ and $\mathcal{Z}_2$ as above.

Finally, from Eq. (15), the full partition function on a torus is

$$\mathscr{Z}(\tilde{\kappa}) \simeq \exp(-MNf_\infty) \frac{q^{2\tilde{\kappa}^2}}{2\eta^2(q)} \sum_{i=1}^{4} p_i \theta_i^2(z, q) \qquad (48)$$

This result does not change when N is an odd integer. Note that $\exp(-MNf_\infty)$ is the bulk term in the partition function, while its coefficient is the $\mathscr{O}(1)$ term, $\mathscr{Z}^{\mathscr{O}(1)}$. The form of $\mathscr{Z}^{\mathscr{O}(1)}$ in the partition function is universal. The only model dependence enters through the anisotropy factor ζ, which modifies the aspect ratio by $s \to s\zeta$ as usual for anisotropic systems in the conformal theory. The same formula has been obtained by Bhattacharjee[20] for the generalized dimer model on a square lattice where horizontal dimers have activity x while vertical dimers have activities 1 and y alternately. This dimer model can be identified as one special case when the dispersion relation is given by

$$\mathscr{E}(k) = 2 \ln\{x \cos(k/2) + [y + x^2 \cos^2(k/2)]^{1/2}\}$$

This dispersion relation satisfies the general properties of $\mathscr{E}(k)$ $(-\pi < k < \pi)$ assumed in Section 2.

The parameter $\tilde{\kappa}$ is related to mismatch between the domain wall separation $l_h = 1/d$ and the system size N. In terms of the bulk domain wall density $d = k_F/\pi$ [Eq. (24)], Eq. (28) becomes $Nd = 2p + 2\tilde{\kappa}$. For convenience, we define a new parameter κ as

$$Nd = n + \kappa \qquad (49)$$

where n is the integer closest to Nd and $-1/2 < \kappa \leqslant 1/2$. The value of the parameter κ indicates how well the system size N matches an integral multiple of the domain wall separation $l_h = 1/d$. We call κ the *mismatch parameter*. The relations between parameters are given as (a) $n = 2p - 1$, $\kappa = 2\tilde{\kappa} + 1$ for $-1 < 2\tilde{\kappa} \leqslant -1/2$, (b) $n = 2p$, $\kappa = 2\tilde{\kappa}$ for $-1/2 < 2\tilde{\kappa} \leqslant 1/2$, (c) $n = 2p + 1$, $\kappa = 2\tilde{\kappa} - 1$ for $1/2 < 2\tilde{\kappa} \leqslant 1$.

The integer n is now shown to be equal to the number of domain walls n_d in the ground state of the quantum Hamiltonian in a finite system. The ground state of the quantum Hamiltonian corresponds to the state of the two-dimensional system with the lowest free energy in the infinite-cylinder limit $M \to \infty$. Two sectors of $n_d = $ even ($\mathscr{Z}_3$) and odd ($\mathscr{Z}_2$) compete for the ground state. Equations (32) and (42) represent the negative of the total free energy for the even and odd sector, respectively, for $\tilde{\kappa} > 0$. Comparing these free energies, we find that the number of domain walls in the ground state is $n_d = 2p$ (even sector) for $0 < 2\tilde{\kappa} \leqslant 1/2$ and $n_d = 2p + 1$ (odd sector) for $2\tilde{\kappa} > 1/2$. Using the relations between n and p in (b) and (c) above, we

identify $n = n_d$. The same result follows for $\tilde{\kappa} < 0$. The domain wall density in finite systems, n_d/N, rarely matches the bulk density d exactly. Thus, there is almost always a deficit (or excess) of a fraction of a domain wall in a finite system. The mismatch parameter κ represents the deficit of domain walls in finite systems. Therefore the free energy difference between the two situations $\kappa = 0$ and $\kappa \neq 0$ represents the free energy of the κ missing domain walls.

Using theta function properties,[22] one can easily show that the partition function (48) is invariant under the transformation $\tilde{\kappa} \to -\tilde{\kappa}$ $(z \to -z)$ and also invariant under the transformation $\tilde{\kappa} \to \tilde{\kappa} - 1/2$ $(z \to z - \frac{1}{2} i\pi s\zeta)$. So the $\mathscr{O}(1)$ term of the partition function is rewritten in terms of the new parameter κ as

$$\mathscr{Z}^{\mathscr{O}(1)}(\kappa) = \frac{q^{\kappa^2/2}}{2\eta^2(q)} \sum_{i=1}^{4} p_i \theta_i^2 \left(\frac{z_\kappa}{2}, q \right) \tag{50}$$

where $z_\kappa = 2z = i\pi s\zeta\kappa$. $\mathscr{Z}^{\mathscr{O}(1)}$ is invariant under the transformation $\kappa \to -\kappa$.

For a given bulk density d [i.e., given m and t in the quantum Hamiltonian (6)], there is a unique value of κ for each system width N. The dependence of κ on N is periodic with period Q when d is a rational P/Q. Otherwise κ is a quasiperiodic function of N. For example, when $d = 1/4$, we have $\kappa = 0$, $1/4$, $1/2$, $-1/4$ corresponding to $N = 0$, 1, 2, 3 (mod 4). So the partition function has different finite-size amplitudes for each N. The thermodynamic limit of the finite-size correction term is not well defined mathematically for irrational d. In Fig. 2, we show how finite-size corrections vary with system size N when (a) $d = 2/7$ and (b) $d = 1/(1 + \sqrt{5})$.

We generalize the above results to twisted (gauge-invariant) boundary conditions. After algebraic manipulations as before, we find

$$\mathscr{Z}^{\mathscr{O}(1)}(\kappa, \phi) = \frac{q^{\kappa^2/2 + 2\phi^2}}{2\eta^2(q)} \sum_{i=1}^{4} p_i \theta_i \left(\frac{z_\kappa}{2} + z_\phi, q \right) \theta_i \left(\frac{z_\kappa}{2} - z_\phi, q \right) \tag{51}$$

where $z_\phi = i\pi s\zeta\phi$. Remarkably, this equation can be rewritten in a simpler form

$$\mathscr{Z}^{\mathscr{O}(1)}(\kappa, \phi) = \frac{q^{\kappa^2/2 + 2\phi^2}}{\eta^2(q)} \theta_3 \left(\frac{z_\kappa}{2}, q^{1/2} \right) \theta_3(2z_\phi, q^2) \tag{52}$$

We checked numerically that the coefficients of the expansion in powers of $q^{1/2}$ in these two equations are identical. We leave it to the interested reader to find an analytical proof of the equivalence. This equivalence plays a crucial role in relating finite-size corrections of the incommensurate phase
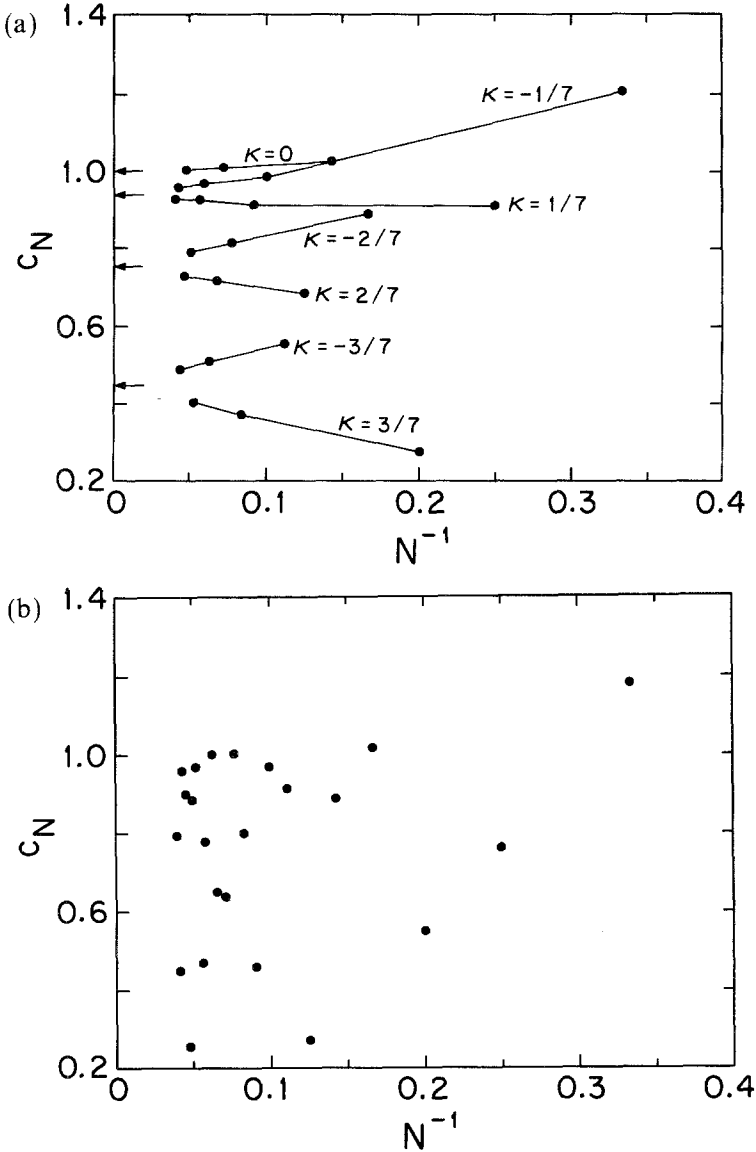
Fig. 2. (a) Numerical data for the FSS amplitudes of the free-fermion model for the domain wall density $d = 2/7$ on an infinite cylinder $(s \to \infty)$ of width N with periodic boundary conditions. c_N is proportional to the FSS amplitudes; $c_N = (6/\pi\zeta) N^2(f_\infty - f_N)$, where ζ is the anisotropy factor $[2 \sin(\pi d)]$, f_N is the free energy for finite systems, and f_∞ is the bulk free energy. Numerical data with the same value of the mismatch parameter κ are linked by lines. Arrows indicate the exact values of the effective conformal charge c_∞ obtained from Eq. (55). (b) Numerical data for an irrational value of the domain wall density, $d = 1/(1 + \sqrt{5})$. There are no data points which share the same value of κ.

and the six-vertex model. The expression in (52) is similar to $\mathscr{L}^{\mathcal{O}(1)}$ of the six-vertex model (or the Coulomb gas).[12,13,21] In fact, when $\kappa = \phi = 0$, Eq. (52) becomes identical to $\mathscr{L}^{\mathcal{O}(1)}$ of the six-vertex model at the free fermion point with periodic boundary conditions, aspect ratio $s\zeta$, and an even number of sites.[13,21] In the next section we explore the relation between Eq. (52) and $\mathscr{L}^{\mathcal{O}(1)}$ of the six-vertex model with nonzero κ and ϕ.

Next consider fixed boundary conditions in the horizontal direction. The allowed wavevectors are $k_j = \pi j/N'$ ($j = 1,..., N$), where $N' = N + 1$ (see Section 2). As in Eq. (27), we define $\alpha' = N'k_F/\pi$ so that $\mathscr{E}(\pi\alpha'/N') = 0$. Let n be the integral part of α' and define δ by $\alpha' = n + 1/2 + \delta$ ($-1/2 \leqslant \delta < 1/2$). The energy $\mathscr{E}(\pi j/N')$ is negative for $j = 1,..., n$ and is positive otherwise, so the number of domain walls in the ground state is $n_d = n$. In terms of the bulk domain wall density $d = k_F/\pi$, we find the relation $Nd = n_d + 1/2 - d + \delta$. Following similar procedures to the case of periodic boundary conditions, we find for the partition function

$$\mathscr{Z}_{\text{fixed}} \simeq \exp\left[-MN'f_\infty + \frac{M\mathscr{E}(0)}{2}\right] q'^{\delta^2}\left[\frac{\theta_3(z', q')}{\eta(q')}\right] \tag{53}$$

where $q' = \exp(-\pi s'\zeta/2)$, $z' = i\pi s'\zeta\delta/2$, and $s' = M/N' = M/(N+1)$. The surface free energy of two surfaces is $f_s = f_\infty - \mathscr{E}(0)/2$.

Now examine the partition function (52) in the infinite-cylinder limit ($s \to \infty$) with the domain wall direction parallel to the infinite-cylinder direction. For large s, theta functions in Eq. (52) may be expanded in terms of small q. Then the free energy

$$f(\kappa, \phi) = f_\infty - (\pi/6)\,\zeta c/N^2 + \cdots \tag{54}$$

where c, the *effective* conformal charge, is given by

$$c = 1 - (3\kappa^2 + 12\phi^2) \tag{55}$$

As discussed before, $\kappa = 0$ is special. At $\kappa = 0$ the exact ground states are realized even in finite systems, i.e., no excess (or deficit) of domain walls is present. The κ-dependent term is interpreted as the excess free energy due to the κ missing domain walls. So κ plays the same role as steps in step boundary conditions in the BCSOS or the Gaussian model, where the height at site $N + 1$ is lower by κ than at site 1. The Gaussian coupling constant K_g takes the free fermion value, $K_g = \pi$.[15] Extensions of our results to general values of K_g will be described in the next section.

Notice that, by replacing the domain wall density d by $d - \kappa/N$ in the bulk free energy f_∞ in Eq. (23), one can obtain precisely the same correction as in the above equation. The finite-size-scaling amplitude $A_{\parallel}$ for this

cylinder is defined as the coefficient of the $\mathcal{O}(1/N^2)$ term, i.e., $A_{\parallel} = (\pi/6)\,\zeta[1 - (3\kappa^2 + 12\phi^2)]$. When $\kappa = 0$ and $\phi = 0$ (periodic boundary conditions), it implies that the conformal charge is $c = 1$ with the anisotropy factor ζ. In general, the FSS amplitude is modified by κ and ϕ as above.

The free energy for fixed boundary conditions, expanded for small q, is

$$f_{\text{fixed}} = f_\infty + f_s/N - (\pi/24)\,\zeta(1 - 12\delta^2)/N^2 + \cdots \tag{56}$$

where δ is given as $Nd = n + 1/2 - d + \delta$ (n is an integer and $-1/2 \leqslant \delta < 1/2$). Notice that the correction to the free energy due to nonzero δ is precisely the same as the correction in Eqs. (54) and (55) due to nonzero κ. At $d = 1/2$, δ represents the deficit of domain walls in finite systems. Elsewhere there exist the extra $d - 1/2$ domain walls in finite systems besides the δ missing domain walls. When $d = 1/2$ and N is even, then $\kappa = \delta = 0$ and the FSS amplitude for fixed boundary conditions is exactly one-quarter of that for periodic boundary conditions as is true in conformally invariant systems.[4]

It is interesting to perform inversion transformations of Eqs. (51) and (52), using the inversion transformation formulas for theta functions.[22] Then the partition function becomes

$$\mathscr{Z}^{\mathcal{O}(1)}(\kappa, \phi) = \frac{1}{2\eta^2(\tilde{q})} \sum_{i=1}^{4} \theta_i\left(\frac{\tilde{z}_\kappa}{2} + \tilde{z}_\phi, \tilde{q}\right) \theta_i\left(\frac{\tilde{z}_\kappa}{2} - \tilde{z}_\phi, \tilde{q}\right)$$

$$= \frac{1}{\eta^2(\tilde{q})}\, \theta_3(\tilde{z}_\phi, \tilde{q}^{1/2})\, \theta_3(\tilde{z}_\kappa, \tilde{q}^2) \tag{57}$$

where $\tilde{q} = \exp(-\pi/s\zeta)$, $\tilde{z}_\kappa = \pi\kappa$, and $\tilde{z}_\phi = \pi\phi$. Notice that the first arguments of theta functions, $\tilde{z}_\kappa$ and $\tilde{z}_\phi$, are now real, in contrast to pure imaginary z_κ and z_ϕ in Eqs. (51) and (52). In the $s \to 0$ infinite-cylinder limit (the domain wall direction is perpendicular to the infinite-cylinder direction), the free energy is expanded for small $\tilde{q}$ as

$$f(\kappa, \phi) = f_\infty - (\pi/6\zeta)/M^2 + \cdots \tag{58}$$

The FSS amplitude for this cylinder is $A_{\perp} = \pi/(6\zeta)$.

There is no discreteness in the domain wall density in this geometry because the domain walls lie perpendicular to the infinite-cylinder direction. Therefore the κ-dependent term disappears. The twisted boundary conditions in the infinite-cylinder direction also do not contribute to the finite-size corrections of the free energy. As usual in conformally invariant systems, the anisotropy factor ζ in the FSS amplitude is placed in

the denominator, in contrast to the orthogonal cylinder geometry in which ζ appears in the numerator. At $\kappa = \phi = 0$, the conformal charge $c = (6/\pi)(A_{\|} A_{\perp})^{1/2}$ is again found to be 1.

4. EXTENSION TO AN INTERACTING FERMION MODEL

In this section we compare the finite-size corrections to the free energy of the free fermion model and the six-vertex model. The mismatch parameter κ and the twist angle ϕ are interpreted in the language of the six-vertex model (or the Coulomb gas). Based on the correspondence between two models, we conjecture an explicit formula for finite-size corrections to the free energy of an interacting fermion model on a torus with a general value of the aspect ratio s. Through Bethe-Ansatz calculations we confirm our conjecture in the infinite-cylinder limit ($s \to \infty$).

Consider the symmetric six-vertex model (or the F model). Boltzmann weights of vertices are given by $\omega_i = a$ ($i = 1, 2, 3, 4$) and $\omega_i = 1$ ($i = 5, 6$) (see Fig. 3). The conventional six-vertex parameter Δ is defined by $\Delta = 1 - 1/(2a^2)$. Configurations of this model are classified by two polarizations, P_1 and P_2. The $\mathcal{O}(1)$ part of the partition function of the six-vertex model with periodic boundary conditions and fixed values of polarizations is the same as in the Gaussian model with step boundary conditions. The relation between the Gaussian coupling constant K_g and the six-vertex parameter Δ is given by[15,23]

$$\Delta = -\cos(\mu) \quad \text{and} \quad K_g = 2(\pi - \mu) \tag{59}$$

Define polarizations P_1 (P_2) by subtracting the number of down-pointing (or left-pointing) arrows from the number of up-pointing (right-pointing) arrows and dividing by 2 (see Section 4 of Ref. 21). We assume that the numbers of vertices in both horizontal and vertical directions N and M are even. Then P_1 and P_2 can take all possible integer values in the thermodynamic limit. So the leading finite-size correction to the partition function of the six-vertex model with periodic boundary condition is

$$\mathcal{Z}_{6V}^{\mathcal{O}(1)} = \sum_{P_1, P_2 \in Z} \mathcal{Z}_g^{\mathcal{O}(1)}(P_1, P_2) \tag{60}$$
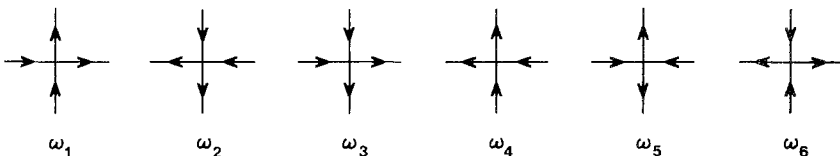
Fig. 3. Vertex configurations of the six-vertex model.

where $\mathscr{L}_g^{\mathcal{O}(1)}(P_1, P_2)$ is the $\mathcal{O}(1)$ part of the partition funtion of the Gaussian model with step boundary conditions of P_1 horizontal steps and P_2 vertical steps. $\mathscr{L}_g^{\mathcal{O}(1)}(P_1, P_2)$ is easily evaluated (see ref. 21). Using the Poisson summation over P_2, we find that the above equation becomes

$$\mathscr{L}_{6V}^{\mathcal{O}(1)} = \frac{1}{\eta^2(q)} \sum_{e,m \in Z} q^{(K_g/2\pi)e^2 + (2\pi/K_g)m^2} \tag{61}$$

where $q = \exp(-\pi s)$. Note that the anisotropy factor is $\zeta = 1$ for the isotropic six-vertex model. The summation variables e and m are integers and are called the electric and magnetic charge, respectively, in the Coulomb gas language.[11,13] The electric charge e is simply the horizontal polarization P_1.

The quantum mechanical version of the six-vertex model is spin-1/2 XXZ Heisenberg chain with the Hamiltonian[15]

$$\mathscr{H}_{XXZ} = -\frac{1}{2} \sum_{n=1}^{N} (\sigma_n^x \sigma_{n+1}^x + \sigma_n^y \sigma_{n+1}^y + \Delta \sigma_n^z \sigma_{n+1}^z) \tag{62}$$

where σ_n^x, σ_n^y, and σ_n^z are the spin-1/2 Pauli matrices at site n. In terms of the raising/lowering operators $\sigma^{\pm} = (\sigma^x \pm i\sigma^y)/2$, the Hamiltonian becomes

$$\mathscr{H}_{XXZ} = \sum_{n=1}^{N} \left[2\Delta \sigma_n^+ \sigma_n^- - (\sigma_n^+ \sigma_{n+1}^- + \sigma_n^- \sigma_{n+1}^+) - 2\Delta \sigma_n^+ \sigma_n^- \sigma_{n+1}^+ \sigma_{n+1}^- - \frac{\Delta}{2} \right] \tag{63}$$

where the third term represents the interaction between domain walls. At $\Delta = 0$ (free-fermion point), the XXZ Hamiltonian becomes identical to the free-fermion Hamiltonian (6) with $m = 0$ and $t = 2$. Notice that, at these values of m and t, the bulk domain wall density is $d = 1/2$. The Gaussian coupling constant K_g takes the free-fermion value π at $\Delta = 0$; see Eq. (59).

Using the definition of the theta function, we rewrite the $\mathcal{O}(1)$ part of the partition function of the free-fermion model, Eq. (52), as

$$\mathscr{L}_{FF}^{\mathcal{O}(1)} = \frac{1}{\eta^2(q)} \sum_{e,m \in Z} q^{(e-\kappa)^2/2 + 2(m-\phi)^2} \tag{64}$$

In the Coulomb gas language, κ and ϕ represent eletric and magnetic defect charges. With periodic boundary conditions, the twist angle is $\phi = 0$ by definition. When the domain wall density is $d = 1/2$ (the value for the symmetric six-vertex model), the mismatch parameter κ takes the value of 0 or 1/2 for N even or odd, respectively. Indeed, we recover the result for the six-vertex model at the free-fermion point ($K_g = \pi$) for N even, Eq. (61),

when $\kappa = \phi = 0$. For N odd, the polarization P_1 $(=e)$ takes half-integer values in Eqs. (60) and (61) and we find the equivalence of $\mathcal{Z}^{\mathcal{O}(1)}$ at $\kappa = 1/2$.

For the six-vertex model, the exact result for $\mathcal{Z}^{\mathcal{O}(1)}$ is known for nonzero Δ ($K_g \neq \pi$), but the domain wall density is always $d = 1/2$. For the free-fermion model, the effect of general values of domain wall density $(d \neq 1/2)$ on $\mathcal{Z}^{\mathcal{O}(1)}$ was explored in the previous section at $\Delta = 0$. So it is natural to study generalized models with both continuously varying domain wall density and domain wall interactions (nonzero Δ). For example, the XXZ chain with domain-wall chemical potential m (or magnetic field) contains both features,

$$\mathcal{H} = \mathcal{H}_{XXZ} + m \sum_{n=1}^{N} \sigma_n^+ \sigma_n^- \tag{65}$$

The chemial potential m controls the domain wall density. This model is a quantum mechanical prototype for physically relevant incommensurate solid phases such as occur in the chiral three-state Potts model and the ANNNI model in two dimensions with a proviso that dislocations are excluded (for a review, see ref. 8).

By comparing the results for the free-fermion model and the six-vertex model in Eqs. (61) and (64), we conjecture the form of the $\mathcal{O}(1)$ partition function for the generalized model

$$\mathcal{Z}^{\mathcal{O}(1)} = \frac{1}{\eta^2(q)} \sum_{e,m \in Z} q^{(K_g/2\pi)(e-\kappa)^2 + (2\pi/K_g)(m-\phi)^2} \tag{66}$$

At $K_g = \pi$ we recover our free-fermion result in Eq. (64). The above conjecture implies that in the interacting-fermion model κ and ϕ still play exactly the same roles as in free-fermion models, i.e., they are electric and magnetic defect charges. There is no interplay between these two defects. The Gaussian coupling constant K_g is related to the correlation function exponent x by $K_g = \pi x$.[8] In free-fermion models, x is always 1, independent of the value of the domain wall density d. In the six-vertex model, x is given by Eq. (59) and d is always 1/2. In the generalized model, K_g is still given by πx, but x now depends both on Δ and d.[9,24]

In the infinite-cylinder limit ($s \to \infty$), the free energy takes the form of Eq. (54) and the effective conformal charge is

$$c = 1 - 6 \left(\frac{K_g}{2\pi} \kappa^2 + \frac{2\pi}{K_g} \phi^2 \right) \tag{67}$$

Both κ and ϕ modify the effective conformal charge to $c = 1 - 12 x_{\kappa,\phi}$, where $x_{n,m} = n^2 K_g / (4\pi) + m^2 \pi / K_g$ is the scaling dimension of the operator

with the spin-wave excitation index n and the vortex excitation index m.[25] This formula has been shown to be correct for the XXZ chain at $d = 1/2$ ($\kappa = 0$ and $1/2$) numerically[26] and analytically.[27]

Interestingly, the conjectured form of the finite-size correction for the generalized model, $\mathscr{L}^{\mathcal{O}(1)}$ in Eq. (66), can be obtained precisely from the $\mathscr{L}^{\mathcal{O}(1)}$ terms of the six-vertex model [Eqs. (60)] by assuming that the possible values of the horizontal polarization are not integers, but rather are shifted by κ from integer values. That is, $P_1 = n - \kappa$ (n is an integer). Up-pointing arrows in six-vertex configurations can be interpreted as domain walls, so $P_1 = n_\uparrow - N/2 = n_d - N/2$, where $n_\uparrow$ is the number of up-pointing arrows in a row of a vertex configuration. As discussed before in the previous section, κ (the shift in P_1) is identified as the (fractional) number of missing domain walls in finite systems. As P_1 corresponds to the electric charge in the Coulomb gas formalism, this shift in P_1 is identical to the electric defect in the Coulomb gas system. Hamer and Batchelor[28] recently observed this effect in the XXZ chain. By investigating the energy spectrum of the $d = 1/2$ sector with extra domain walls, they found that the free energy with n extra domain walls is given by Eq. (67) after replacing κ by n.

The twist angle ϕ can be also interpreted in the six-vertex model language. The presence of the nonzero twist angle does not change the total number of domain walls in the system, but does change the hopping probability of domain walls at the boundary (the seam). That is, the hopping from site $n = N$ to $n = 1$ (or vice versa) collects an extra phase factor $\exp(i2\pi\phi)$ [$\exp(-i2\pi\phi)$]; see Eq. (17). In the Coulomb gas formulation, these phase factors correspond to boundary charges $2\pi\phi$ and $-2\pi\phi$ at the top and bottom of the infinite cylinder ($s = \infty$). The energy density of this condenser contributes to the finite-size-saling amplitude of the free energy and modifies the effective conformal charge accordingly. Substituting 2ϕ for α in Eq. (3.16) of ref. 21, we recover our Eq. (67) at $\kappa = 0$. On a torus it can be derived from Eq. (4.9) of ref. 21 that the leading finite-size correction to the partition function is

$$\mathscr{L}^{\mathcal{O}(1)} = \sum_{P_1, P_2} \mathscr{L}_g^{\mathcal{O}(1)}(P_1, P_2) \cos(2\pi\phi P_2)$$

This is an equivalent expression to our Eq. (66) at $\kappa = 0$.

We tested our conjecture through Bethe-Ansatz calculations for the model Hamiltonian in Eq. (65) in the infinite-cylinder limit ($s \to \infty$). The extra mass term (magnetic-field term) does not alter the Bethe-Ansatz equations for allowed wavevectors k,[26,27]

$$Nk_j = 2\pi(I_j + \phi) - \sum_{l=1}^{n} \Theta(k_j, k_l) \tag{68}$$

where

$$\Theta(k, k') = 2 \tan^{-1} \left[\frac{\Delta \sin[(k - k')/2]}{\cos[(k + k')/2] - \Delta \cos[(k - k')/2]} \right] \quad (69)$$

n is the number of up-pointing arrows (domain walls), and $I_1, I_2,..., I_n = -(n-1)/2, -(n-1)/2 + 1,..., (n-1)/2$. These equations are valid when the total number of sites N is even and can easily be altered for odd N. The energy density is

$$\varepsilon = -\frac{\Delta}{2} + \frac{1}{N} \sum_{j=1}^{n} [2\Delta + m - 2\cos(k_j)] \quad (70)$$

We find the ground-state energy for a given Δ and m by minimizing the energy ε with respect to integer n. The ground-state energy of the quantum chain is exactly the same (up to finite-size corrections) as the free energy of the two-dimensional system in the infinite-cylinder geometry ($s \to \infty$).

We solve the above equations numerically for different system sizes N and twist angles ϕ. The form of the FSS amplitudes in Eqs. (54) and (67) agrees with our numerical calculations for different values of Δ and m. In particular, the FSS amplitudes contain no dependence on κ or ϕ other than quadratic terms, there are no cross terms (no interplay between two different defects), and the coefficients of κ and ϕ have an inverse relation. Tables I and II list a sampling of numerical values of $x = K_g/\pi$ and ζ obtained from our calculations. Notice that x takes the free-fermion value 1 in the $d = 0$ limit in addition to the obvious $\Delta = 0$ limit.

Table I. Numerical Values of Correlation-Function Critical Exponent $x = K_g/\pi$ for Several Different Values of $\mu = \cos^{-1}(-\Delta)$ and Domain Wall Density d[a]

	$x(\mu, d)$				
μ	$d = 1/2$	$d = 1/3$	$d = 1/4$	$d = 1/5$	$d = 0$
$2\pi/3$	2/3	0.6875	0.7178	0.7460	1
$\pi/2$	1	1	1	1	1
$\pi/3$	4/3	1.2474	1.1839	1.1451	1
$\pi/6$	5/3	1.3938	1.2780	1.2143	1
0	2	1.4404	1.3062	1.2346	1

[a] For $d = 1/2$, the chemical potential is $m = 0$. In general, m depends on both μ and d. For example, the value of the chemical potential corresponding to the domain wall density $d = 1/5$ is $m = 2.542609740...$ for $\mu = \pi/3$ and $m = 3.238555355...$ for $\mu = \pi/6$.

Table II. Numerical Values of Anisotropy Factors ζ
for Several Different Values of μ and d^a

μ	$\zeta(\mu, d)$				
	$d = 1/2$	$d = 1/3$	$d = 1/4$	$d = 1/5$	$d = 0$
$2\pi/3$	$3\sqrt{3}/4$	1.167169	1.001707	0.869107	0
$\pi/2$	2	$\sqrt{3}$	$\sqrt{2}$	$2\sin(\pi/5)$	0
$\pi/3$	$3\sqrt{3}/2$	2.136533	1.665800	1.342585	0
$\pi/6$	3	2.348867	1.787000	1.419378	0
0	π	2.411585	1.822242	1.441474	0

^{a} See footnote to Table I.

We also study the above Bethe-Ansatz equations perturbatively in two simple limits, i.e., the $d = 0$ limit and $\Delta = 0$ limit. At $d = 0$ or $\Delta = 0$, the wavevectors k have a uniform distribution of the free-fermion type. So one can investigate the Bethe-Ansatz equations analytically near these limits. After lengthy but straightforward algebra, it is found again that the conjectured form of the FSS amplitudes is correct. Near $\Delta = 0$ we obtain

$$m = 2\cos(\pi d) - 2\Delta \left[1 - 2d + \frac{1}{\pi}\sin(2\pi d) \right] + \cdots$$

$$\zeta = 2\sin(\pi d) - \frac{4\Delta}{\pi}\sin^2(\pi d) + \cdots \tag{71}$$

$$x = 1 - \frac{2\Delta}{\pi}\sin(\pi d) + \cdots$$

for arbitrary d. Near $d = 0$ we obtain

$$m = 2(1 - \Delta) - \pi^2 d^2 + \frac{8\pi^2}{3} d^3 \frac{\Delta}{1 - \Delta} + \cdots$$

$$\zeta = 2\pi d - 4\pi d^2 \frac{\Delta}{1 - \Delta} + \cdots \tag{72}$$

$$x = 1 - 2d \frac{\Delta}{1 - \Delta} + \cdots$$

for arbitrary Δ. The bulk free energy is given by the equation $m = -(\partial f_\infty)/(\partial d)$. At $m = 2(1 - \Delta)$, the domain wall density vanishes and the commensurate–incommensurate transition occurs.

5. DISCUSSIONS

In summary, we derived the FSS amplitudes of incommensurate phases and found that they obey laws of conformal invariance, but competition between system size and domain wall separation generates some defects (missing domain walls) for finite systems with periodic boundary conditions. Due to these defects, numerical data for the FSS amplitudes in incommensurates phases appear superficially as if they do not converge in the thermodynamic limit. This work explains why the FSS amplitudes are scattered, and leads to a systematic way of analyzing data.

Our theory applies to a wide class of systems describable in terms of noninteracting domain walls, e.g., certain dimer models[20] and tiling models of quasicrystals.[17] A set of general assumptions regarding the form of the domain wall dispersion relation appears to guarantee universality, and we also extend our theory to systems of interacting domain walls. Our results may be useful for analyzing numerical data from transfer matrix and Monte Carlo calculations for these systems. For instance, in systems for which the bulk density is rational, $d = P/Q$, it is conventional to study only lattices whose widths N are integral multiples of the denominator Q to ensure smooth convergence to the thermodynamic limit. Our formula (66) allows data for all lattice sizes to be systematically included. This is especially important when the domain wall density d is a high-order rational or is irrational, since in these cases it may not be practical to study systems of size proportional to the denominator Q. Unfortunately, knowledge of the exact bulk density may not be available for an incommensurate system at an arbitrary chemical potential. In this case the density (which determines κ) must be included as an extra fitting parameter which would not be needed in ordinary commensurate systems.

Another possible approach is to utilize free boundary conditions and thereby avoid the κ effect. The κ effect arises because conservation of domain walls by periodic (or gauge-invariant) boundary conditions forces the number of domain walls in the ground state to be an integer. In systems with free boundaries, domain walls can pass into or out of the system, so the average number of domain walls in the ground state need not be an integer. Thus, we expect that $c = 1$ exactly without any κ effect in terms of order $1/N^2$ in the free energy density. But one must endure the appearance of nonuniversal surface terms in the free energy. Nevertheless, this may not cause as much trouble as the κ effect does. We suggest that free boundary conditions may be an especially suitable choice for studies of incommensurate systems. Our study of these free boundary conditions in a random tiling model has been published elsewhere.[17]

In this work we did not include dislocations at all. Dislocations are

present in the chiral three-state Potts model and the ANNNI model in two dimensions. An important generalization of this work is to study how the FSS amplitudes change in the presence of dislocations. The main question is whether the κ effect disappears or not. Dislocations can break the conservation law on the number of domain walls and so may remove the κ effect. However, there can be some conservation laws left which are not broken by the presence of special types of dislocations, so the κ effect might survive. Another aspect which we did not address in this paper is the FSS behavior near the commensurate–incommensurate transition where anisotropic scaling sets in (the anisotropy factor $\zeta \to 0$) and conformal invariance disappears. This anisotropic FSS behavior was studied extensively by Bhattacharjee and Nagle for generalized dimer models.[20] Surface effects on the anisotropic finite-size scaling are currently under investigation and the results will appear elsewhere.[29]

ACKNOWLEDGMENTS

REFERENCES

1. M. N. Barber, in *Phase Transitions and Critical Phenomena*, Vol. 8, C. Domb and J. L. Lebowitz, eds. (Academic, New York, 1983).
2. V. Privman, in *Finite Size Scaling and Numerical Simulations of Statistical Systems*, V. Privman, ed. (World Scientific, Singapore, 1990).
3. J. L. Cardy, *Finite Size Scaling* (North-Holland, Amsterdam, 1988).
4. H. W. Blöte, J. L. Cardy, and M. P. Nightingale, *Phys. Rev. Lett.* **56**:742 (1986); I. Affleck, *Phys. Rev. Lett.* **56**:746 (1986).
5. J. L. Cardy, in *Phase Transitions and Critical Phenomena*, Vol. 11, C. Domb and J. L. Lebowitz, eds. (Academic, New York, 1987).
6. M. P. Nightingale and H. W. J. Blöte, *J. Phys. A* **16**:L657 (1983).
7. H. Park and M. den Nijs, *J. Phys. A* **22**:3663 (1989); J.-S. Wang, R. H. Swendsen, and R. Kotecký, *Phys. Rev. Lett.* **63**:109 (1989); H. Park and M. Widom, *Phys. Rev. Lett.* **63**:1193 (1989); H. Park, *J. Phys. A* **23**:1789 (1990).
8. M. den Nijs, in *Phase Transitions and Critical Phenomena*, Vol. 12, C. Domb and J. L. Lebowitz, eds. (Academic, New York, 1988).
9. N. M. Bogoliubov, A. G. Izergin, and N. Yu Reshetikhin, *J. Phys. A* **20**:5361 (1987).
10. F. Woynarovich, H.-P. Eckle, and T. T. Truong, *J. Phys. A* **22**:4027 (1989).
11. B. Nienhuis, in *Phase Transitions and Critical Phenomena*, Vol. 11, C. Domb and J. L. Lebowitz, ed. (Academic, New York, 1987).
12. C. B. Thorn, *Phys. Rep.* **67**:171 (1980).
13. C. Itzykson and J. B. Zuber, *Nucl. Phys. B* **275**:580 (1986); P. di Francesco, H. Saleur, and J. B. Zuber, *J. Stat. Phys.* **49**:57 (1987).
14. H. Park and M. Widom, *Phys. Rev. Lett.* **64**:1076 (1990).

15. R. J. Baxter, *Exactly Solvable Models in Statistical Mechanics* (Academic, London, 1982).
16. F. C. Alcaraz, M. N. Barber, M. T. Batchelor, R. J. Baxter, and G. R. W. Quispel, *J. Phys. A* **20**:6397 (1987).
17. W. Li, H. Park, and M. Widom, *J. Phys. A* **23**:L573 (1990).
18. V. L. Pokrovsky and A. L. Talapov, *Phys. Rev. Lett.* **42**:65 (1979).
19. A. E. Ferdinand, *J. Math. Phys.* **8**:2332 (1967); A. E. Ferdinand and M. E. Fisher, *Phys. Rev.* **185**:832 (1969).
20. S. M. Bhattacharjee, Ph. D. thesis, Carnegie-Mellon University, Pittsburgh, Pensylvania (1984); S. M. Bhattacharjee and J. F. Nagle, *Phys. Rev. A* **31**:3199 (1985).
21. H. Park and M. den Nijs, *Phys. Rev. B* **38**:565 (1988).
22. Bateman Manuscript Project, *Higher Transcendental Functions* (McGraw-Hill, New York, 1953), Vol. 2.
23. E. H. Lieb, *Phys. Rev. Lett.* **18**:1046 (1967).
24. F. D. M. Haldane, *Phys. Rev. Lett.* **45**:1358 (1980).
25. L. P. Kadanoff and A. C. Brown, *Ann. Phys.* (N.Y.) **121**:318 (1979).
26. F. C. Alcaraz, M. N. Barber, and M. T. Batchelor, *Phys. Rev. Lett.* **58**:771 (1987); *Ann. Phys.* (N.Y.) **182**:280 (1988).
27. C. J. Hamer, *J. Phys. A* **18**:L1133 (1985); **19**:3335 (1986).
28. C. J. Hamer and M. T. Batchelor, *J. Phys. A* **21**:L173 (1988).
29. W. Li and H. Park, submitted to *J. Phys. A* (1990).